Res Chem Intermed
https://doi.org/10.1007/s11164-018-3354-8

Synthesis and characterization of novel binuclear task-specific ionic liquid: an efficient and sustainable sulfonic-functionalized ionic liquid for one-pot synthesis of xanthenes

Nader Ghaffari Khaligh[1,2]

Received: 5 September 2017 / Accepted: 24 February 2018

Abstract A new binuclear sulfonic-functionalized ionic liquid was synthesized in two steps and its dual solvent-catalytic activity was studied for the synthesis of a variety of xanthenes under mild conditions. The simple experimental and sustainable procedure, good yield of the desired products within short reaction times, and recyclability of the ionic liquid are some advantages of the present strategy, and the current work shows the great importance of task-specific ionic liquids in organic synthesis.

Keywords Binuclear sulfonic-functionalized ionic liquid · Task-specific ionic liquid · Dual solvent-catalyst properties · Xanthene · Sustainable protocol

Introduction

Ionic liquids (ILs) can function as alternative solvents, catalysts and extracting agents due to environmental perspectives including low vapor pressure, thermal and chemical stability, high ionic conductivity, tunable polarity, designable properties, immiscibility with some organic solvents, simplified separation of products and potential reusability [1–3]. The majority of ILs reported for organic transformations and catalysts have focused on imidazole or pyridine-based derivatives [4, 5]. Brönsted acidic ILs (BAILs) containing SO_3H-functionalized on an imidazole ring with an acidic counter-anion and protonated imidazolium cation have been known

✉ Nader Ghaffari Khaligh
ngkhaligh@gmail.com; ngkhaligh@um.edu.my

[1] Research House of Professor Reza, Education Guilan, District 1, Rasht 41569-17139, Iran

[2] Nanotechnology and Catalysis Research Center, 3rd Floor, Block A, Institute of Postgraduate Studies, University of Malaya, 50603 Kuala Lumpur, Malaysia

Published online: 06 March 2018

to show dual solvent-catalyst properties with satisfactory conversion rates and selectivity for multicomponent reactions [6–11]. Nowadays, ILs are used as an unconventional media for sustainable organic synthesis that allows selective separation of the desired products and catalysts in different phases, thus evading tedious and overpriced procedures which consume high volumes of toxic and volatile organic solvents. In this perspective, designing organic reactions in IL media is another attractive area in green chemistry [12, 13]. ILs can be often recovered and reused. Often, an IL can be removed by water from the organic products using a simple workup. When a precious metal catalyst is used in the reaction, this procedure cannot be performed. In another approach, the organic products can be extracted by nonpolar organic solvents and remaining IL can be concentrated and then directly recharged with new reactants for another run.

Xanthene dyes are widely utilized as sensor probes for visualization of biomolecules due to high fluorescence quantum yield and high molar extinction coefficient [14–16]. Also, natural and synthetic xanthene and benzoxanthene derivatives are known to associate with potential biological and pharmaceutical activities [17–23]. These significant properties cause a continuous interest in the synthesis of xanthene derivatives and, consequently, there are numerous reports on their synthesis in the literature [24–34]. Xanthenes are often prepared based on the three-component condensation in the presence of a Brönsted or Lewis acid. Lewis acids are often decomposed or deactivated in the presence of moisture and cannot be recovered and reused, and the residues of Lewis acids can cause environmental problems [35]. Also, in some reported procedures, disadvantages are observed, such as low yields, slow rate of reaction, use of very expensive catalysts, by-product formation, use of an excess of reagents/catalysts, use of toxic organic solvents, corrosion effects, waste metal and acid pollution problems. Therefore, the scope for development of a safer, more convenient and sustainable protocol for the synthesis of xanthenes persists.

In pursuit of our studies on the preparation of new sulfonic-functionalized acidic ILs and their applications as solvent or catalyst in a variety of organic transformations [36–41], herein, a new binuclear task-specific IL (TSIL) was synthesized and its structure was characterized by Fourier transform infrared (FTIR), high-performance liquid chromatography mass spectrometry (HPLC-MS) and ^{1}H and ^{13}C nuclear magnetic resonance (NMR). The physical properties of the new IL were determined and its dual solvent-catalytic activity was investigated for the synthesis of symmetric and unsymmetric xanthenes under mild conditions.

Experiment

Materials

Unless specified, all chemicals were analytical grade and purchased from Merck, Aldrich and Fluka Chemical Companies and used without further purification. Products were characterized by their physical constant and FTIR, NMR and elemental analysis. The purity determination of the substrates and reaction

monitoring were accompanied by thin-layer chromatography (TLC) using silica gel SIL G/UV 254 plates.

Instrumentation

The purity determination and mass spectrometry [MS; electrospray ionization (EI)] data of the products were accomplished by gas chromatography–MS (GC–MS) on an Agilent 6890 N GC system with a 5973 N mass selective detector under 70-eV conditions. The FT-IR spectra were recorded on a Perkin Elmer 781 Spectrophotometer in the range of 4000–400 cm^{-1} using KBr pellets and neat film for solid and liquid samples, respectively. In all cases, the ^{1}H and ^{13}C NMR spectra were recorded with Bruker Avance III 600- and 400-MHz instruments. All chemical shifts are quoted in parts per million (ppm) relative to tetramethylsilane (TMS) using deuterated solvent. Microanalyses were performed on a Perkin-Elmer 240-B microanalyzer. Melting points were recorded on a Büchi B-545 apparatus in open capillary tubes. The HPLC-MS of the products were recorded using an Agilent 6560 iFunnel Q-TOF LC–MS instrument. Thermogravimetric/differential thermal analysis (TG/DTA) curves were obtained with the use of a Mettler Toledo thermogravimetric analyzer/scanning differential thermal analyzer (TGA/SDTA) 851e. The measurements were taken in an Al_2O_3 crucible with a sample mass of 5.12 mg under nitrogen atmosphere (30 mL min^{-1}).

Synthesis of 1,1′-(1,4-butanediyl)bis(imidazole)

Sodium hydride (60%) dispersion in mineral oil (0.4 g, 10 mmol) was slowly added to a flask containing imidazole (0.68 g, 10 mmol) and ground at room temperature for 2 h. 1,4-Dichlorobutane (0.55 mL, 5 mmol) was added, and the mixture was stirred at room temperature overnight. The resulting liquid was poured into 5 mL of water. A white solid formed immediately which weighed 0.94 g (98%) after drying and had the following properties: mp 83–86 °C; IR (KBr): ν_{max} = 3384, 3111, 2925, 1669, 1505, 1463, 1440, 1394, 1378, 1281, 1238, 1108, 1081, 917, 824, 735, 730, 660, 628 cm^{-1}; ^{1}H NMR (600 MHz, DMSO-d_6) δ = 7.61 (s, 2H), 7.13 (t, J = 1.2 Hz, 2H), 6.88 (t, J = 1.02 Hz, 2H), 3.96 (t, J = 6.5 Hz, 4, N–CH_2), 1.60–1.63 (m, 4, –CH_2CH_2–) ppm; ^{13}C NMR (150 MHz, DMSO-d_6) δ = 137.66, 128.86, 119.68, 45.74, 28.13 ppm; MS (ESI): calcd. for $C_{10}H_{15}N_4$: 191.1291, found: 191.1313 and MS (ESI): calcd. for $C_{10}H_{14}N_4Na$: 213.1111, found: 213.1126.

Synthesis of 1,1′-butylenebis(3-sulfo-3H-imidazol-1-ium) chloride (BBSIC)

Chlorosulfonic acid (0.30 mL, 4.4 mmol) was added dropwise to 0.38 g of 2.0 mmol 1,1'-(1,4-butanediyl)bis(imidazole)—BBI—in dry CH_2Cl_2 (2 mL). The reaction mixture was stirred at room temperature for 6 h, and formed two phases; the upper phase was decanted and excess solvent was removed under vacuum evaporation. The resulting colorless liquid was weighed 0.83 g (98%) after drying and had the following properties: IR (KBr): ν_{max} = 3384, 3111, 2925, 1669, 1505, 1463, 1440, 1394, 1378, 1281, 1238, 1108, 1081, 917, 824, 735, 730, 660,

628 cm^{-1}; ^1H NMR (600 MHz, DMSO-d_6) δ = 7.61 (s, 2H), 7.13 (t, J = 1.2 Hz, 2H), 6.88 (t, J = 1.02 Hz, 2H), 3.96 (t, J = 6.5 Hz, 4, N–CH_2), 1.60–1.63 (m, 4, –CH_2CH_2–) ppm; ^{13}C NMR (150 MHz, DMSO-d_6) δ = 28.14, 45.74, 119.68, 128.86, 137.66 ppm; MS (ESI): calcd. for $C_{10}H_{15}N_4O_6S_2$: 351.0433, found: 351.2512.

Physical and spectral data of new products

9-(Furan-2-yl)-3,3,6,6-tetramethyl-3,4,5,6,7,9-hexahydro-2H-xanthene-1,8-dione (**3f**) mp. 164–166 °C; FTIR (KBr) ν_{max}=3064, 2887, 1730, 1670, 1606, 1465, 1350, 1200, 1182, 1138, 1013 cm^{-1}; ^1H NMR (400 MHz, $CDCl_3$) δ = 7.13 (d, J = 7.6 Hz, 1H), 6.18–6.16 (m, 2H), 4.94 (s, 1H), 2.43 (s, 4H), 2.23 (2, 4H), 1.08 (s, 6H), 1.01 (s, 6H) ppm; ^{13}C NMR (100 MHz, $CDCl_3$) δ = 192.4, 164.8, 142.4, 138.6, 116.2, 115.2, 111.2, 50.9, 40.1, 32.3, 29.0, 28.2 ppm; MS (ESI): m/z = $[M + H]^+$ 341.

9-(Thiophene-2-yl)-3,3,6,6-tetramethyl-3,4,5,6,7,9-hexahydro-2H-xanthene-1,8-dione (**3g**) mp. 147–149 °C; FTIR (KBr) ν_{max}=3140, 2924, 1715, 1650, 1618, 1462, 1346, 1208, 1170, 1118, 1010 cm^{-1}; ^1H NMR (400 MHz, $CDCl_3$) δ = 7.31 (dd, J = 7.4 and 1.6 Hz, 1H), 6.83 (d, J = 7.6 Hz, 1H), 6.56 (d, J = 7.4 Hz, 1H), 4.61 (s, 1H), 2.41 (s, 4H), 2.11 (s, 4H), 1.19 (s, 6H), 1.18 (s, 6H) ppm; ^{13}C NMR (100 MHz, $CDCl_3$) δ = 196.2, 162.8, 148.2, 126.7, 125.4, 123.4, 115.3, 50.8, 40.9, 32.2, 29.3, 27.4 ppm; MS (ESI): m/z = $[M + H]^+$ 357.

9-(2-Hydroxy-4,4-dimethyl-6-oxocyclohex-1-enyl)-3,3-dimethyl-2,3,4,9-tetrahydro-1H-xanthen-1-one (**3i**) m.p. 190 °C (dec.); FTIR (KBr) ν_{max}=3181, 2955, 2932, 2870, 1645, 1594, 1374, 1232 cm^{-1}; ^1H NMR (400 MHz, $CDCl_3$) δ = 10.48 (s, 1H), 7.18–7.05 (m, 4H), 2.59–2.33 (m, 6H), 4.68 (s, 1H), 1.97 (d, 2H, J = 4.8 Hz), 1.14 (s, 3H), 1.04 (s, 3H), 1.01 (s, 6H) ppm; ^{13}C NMR (100 MHz, $CDCl_3$) δ = 201.0, 196.5, 170.7, 169.1, 151.1, 128.0, 127.5, 124.6, 124.3, 118.3, 115.7, 111.1, 50.6, 49.9, 43.2, 41.6,32.3, 30.9, 29.9, 29.2, 27.8, 27.2, 26.5 ppm; MS (ESI): m/z = $[M + H]^+$ 367.19.

9-(2,4-Dimethyl-phenyl)-3,3,6,6-tetramethyl-3,4,5,6,7,9-hexahydro-2H-xanthene-1,8-dione (**3j**) mp. 210–212 °C; FTIR (KBr) ν_{max}=2957, 1660, 1465, 1350, 1200, 1162, 1138, 1013, 854 cm^{-1}; ^1H NMR (400 MHz, $CDCl_3$) δ = 7.34 (d, J = 8.4 Hz, 1H), 6.42 (d, J = 9.2 Hz, 1H), 6.32 (s, 1H), 4.77 (s, 1H), 2.74 (s, 3H), 2.47 (s, 3H), 2.43 (d, J = 17.6 Hz, $H_\alpha CH_\beta$, 2H), 2.35 (d, J = 17.6 Hz, $H_\alpha CH_\beta$, 2H), 2.21 (d, J = 16.4 Hz, $H_\alpha CH_\beta$, 2H), 2.16 (d, J = 16.4 Hz, $H_\alpha CH_\beta$, 2H), 1.09 (s, 6H), 0.95 (s, 6H) ppm; ^{13}C NMR (100 MHz, $CDCl_3$) δ = 196.4, 161.9, 159.6, 158.4, 132.7, 123.4, 116.2, 50.9, 40.1, 32.3, 29.0, 28.2, 21.0, 19.4 ppm; MS (ESI): m/z = $[M + H]^+$ 378.

9,9-Dimethyl-12-thiophen-2yl-8,9,10,12-tetrahydro-benzo[a]xanthene-11-one (**3v**) m.p. 175–177 °C; FTIR (KBr) ν_{max}=2920, 1585,1371,1216,1188 cm^{-1}; ^1H NMR (400 MHz, $CDCl_3$) δ = 8.14 (d, J = 8.8 Hz, 1H), 7.82–7.76 (m, 2H), 7.54–7.50 (m, 1H), 7.44–7.40 (m, 1H), 7.33 (d, J = 8 Hz, 1H), 6.97–6.95 (m, 1H),

6.72–6.69(m, 2H), 6.66 (s, 1H), 3.03 (d, J = 16.8 Hz, CH_2CO), 2.83 (d, J = 16.8 Hz, CH_2CO, 1H), 2.62 and 2.60 (AB system, J = 18.1 Hz, CH_aCH_bCO, 2H), 1.11 (s, 3H), 1.02 (s, 3H) ppm; ^{13}C NMR (100 MHz, $CDCl_3$) δ = 201.6, 162.0, 147.5, 147.2, 131.5, 131.0, 129.0, 128.4, 127.2, 125.6, 125.2, 123.9, 123.7, 123.5, 118.2, 60.8, 43.2, 33.1, 32.4, 29.2, 26.4 ppm; MS (ESI): m/z = $[M + H]^+$ 361.12.

Results and discussion

Synthesis of 1,1′-butylenebis(3-sulfo-3H-imidazol-1-ium) chloride nd the characterization of its structure

1,1′-Butylenebis(3-sulfo-3H-imidazol-1-ium) chloride (BBSIC) was prepared in two steps (Scheme 1). In the first step, two equivalents of imidazole were alkylated by one equivalent of 1,4-dichlorobutane in the presence of two equivalent sodium hydride as a base reagent at room temperature. The resulting white solid BBI then was transformed into BBSIC using two equivalent neat chlorosulfonic acids as the sulfonating reagent in CH_2Cl_2 at room temperature overnight. The resulting IL was isolated as a viscous colorless liquid. The structure of BBSIC was confirmed by FTIR, HRMS (ESI), ^1H and ^{13}C NMR.

FTIR spectra of BBSIC are presented in Fig. 1. The broad absorption centered at 3401 cm^{-1} is assigned to O–H stretching vibration of the hydroxyl groups in the sulfonic moiety and the moisture absorbed by the sample. The C–H stretching vibrations of BBSIC were observed at 3144, 2925 and 2854 cm^{-1} which are the characteristic region for the ready identification of C–H stretching vibrations [42, 43]. The bands between 1500 and 1630 cm^{-1} in the title compound are due to C=C and C=N stretching vibrations [44]. The C–H deformation bands were assigned to the peak at 1292 cm^{-1}. The identification of C–N stretching frequency is a very difficult task since the mixing of bands is possible in this region; hence, the FTIR bands at 1455 and 1408 cm^{-1} have been designated to C–N stretching modes of vibrations [45]. FTIR bands at 635, 614 and 588 cm^{-1} have been designated to ring deformation out-of-plane bending. The C–H out-of-plane-bending peaks observed at 1048, 996, 949, 878 and 758 cm^{-1} can be assigned to C–H in-plane bending [44].

The SO_2 asymmetric and symmetric vibrations are observed in the range 1250–1100 cm^{-1} as strong bands in the FTIR spectrum [46]. The sharp peak at 1048 cm^{-1} can be assigned to S–OH bending by comparison with the bending vibration in a variety of the sulfonic acid-functionalized compounds [47]. A series of the broad and strong bands are observed in the region 1160–1000 cm^{-1} due to the S–OH stretching vibrations for the sulfonic acid groups [48, 49]. BBSIC exhibits N–

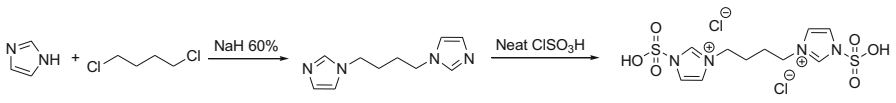

Scheme 1 Synthesis of 1,1′-butylenebis(3-sulfo-3H-imidazol-1-ium) chloride

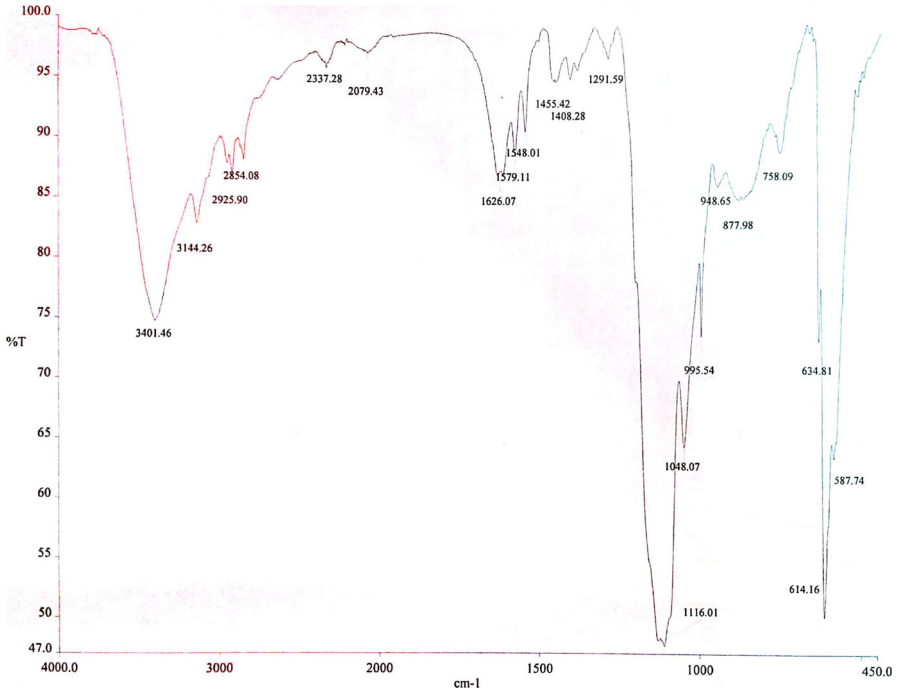

Fig. 1 FTIR spectra of 1,1′-butylenebis(3-sulfo-3*H*-imidazol-1-ium) chloride

S stretching vibrational absorption in the region 950–878 cm^{-1} as a series of the medium-intensity bands [50].

^{1}H NMR spectra of BBSIC in DMSO-d_6 gave sharp signals (Fig. 2). Acidic hydrogen gave a broadened singlet centered at 3.66 ppm, whose shift displacement indicates that the acidic hydrogen is involved in the strong hydrogen bonds in DMSO-d_6. BBSIC contains a total of three aromatic protons attached to an imidazole ring and eight aliphatic protons, which gave a set of three well-resolved signals at 9.16, 7.79 and 7.69 ppm, and a set of two well-resolved signals at 4.25 and 1.85–1.76 ppm, respectively. Of these, one peak was displaced downfield (9.16) and can be assigned to an imidazole ring hydrogen viz. H–C_2. The protons H–C_4 and H–C_5 of the imidazole ring were observed at 7.79 ppm and 7.69 ppm as a pseudotriplet (doublet–doublet) with the same coupling constant ^{4}J = 1.5 and ^{2}J = 1.5 Hz, respectively. One signal was displaced downfield (4.26 ppm) and can be assigned to the protons of the alkyl group N–$C\underline{H}_2$ since their multiplicities correspond to a triplet (t) with coupling constant ^{3}J = 5.9 Hz. Another signal was observed at 1.81–1.78 ppm as a multiplet and can be assigned to the protons alkyl N–CH_2–$C\underline{H}_2$. ^{13}C NMR experiment displays one signal for each of five carbon atoms in the structure of BBSIC with chemical shifts of 135.64, 122.45 and 120.38 ppm for imidazole ring viz., C_2, C_4, and C_5, respectively; and 48.14 ppm for N–$\underline{C}H_2$ and 26.66 ppm for N–CH_2–$\underline{C}H_2$ for carbon atoms in the butane chain, respectively.

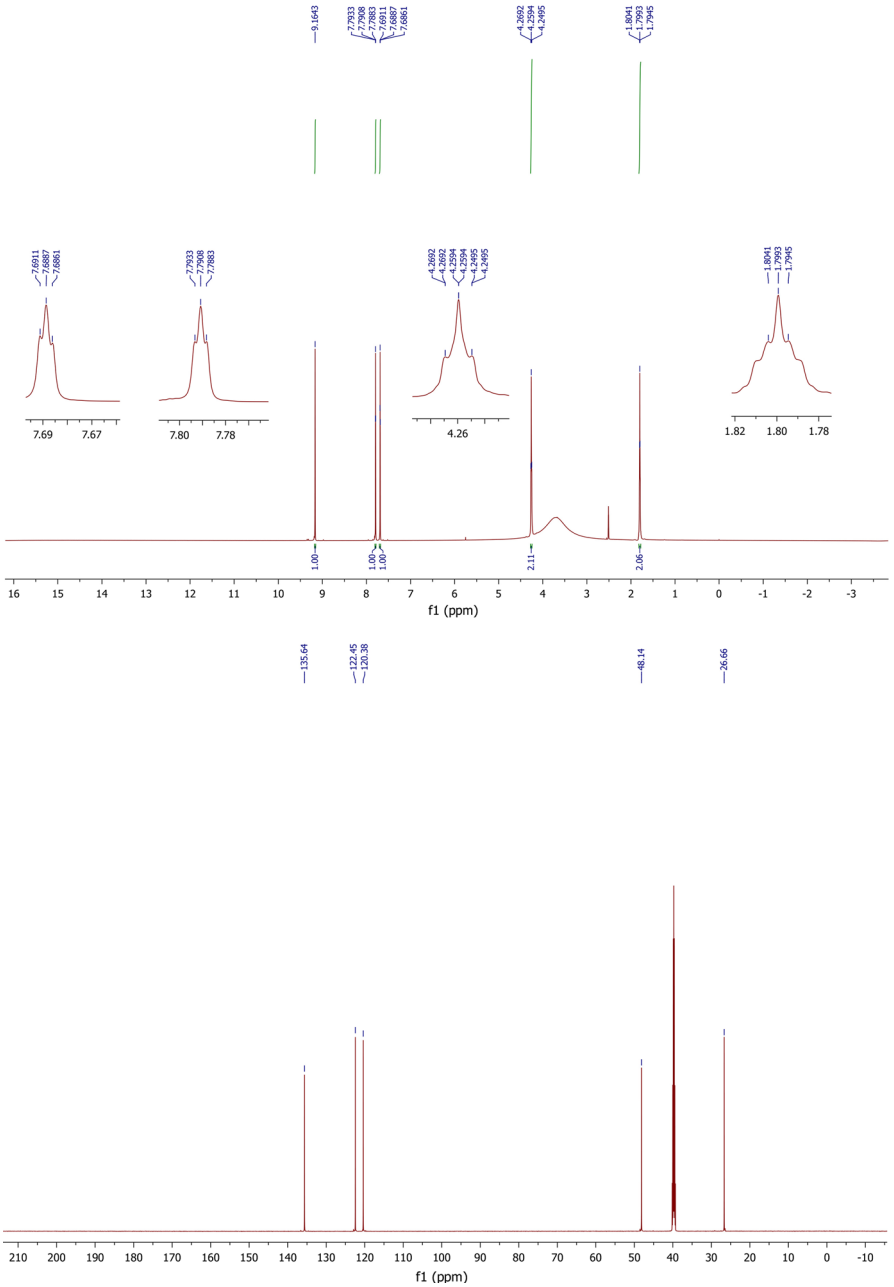

Fig. 2 ^{1}H and ^{13}C NMR spectra of 1,1′-butylenebis(3-sulfo-3*H*-imidazol-1-ium) chloride

The viscosity of BBSIC was 302 ± 2 cPa at 27 ± 1 °C. The hydrophilic ILs readily absorb moisture from the atmosphere during storage; therefore, the exact amount of water in BBSIC was determined by Karl Fisher (KF) titration, using a Metrohm 831 KF coulometer in conditions of ambient humidity and room temperature. The conditions of temperature, pressure and drying time were 100 °C, 80 mbar and 12 h, respectively. The water content in BBSIC was 0.28 ± 0.02 wt.%. The 0.01 molar solutions of BBSIC were prepared in the deionized water and the pH readings were recorded with a pH meter (F-71, LAQUA-HORIBA Scientific) at 27 ± 1 °C. The pH of 0.01 M aqueous solution of BBSIC was 2.9 ± 0.1. The standard deviation was obtained from three replicate determinations on the different three days. The new IL BBSIC was immiscible with ethyl acetate, n-hexane and toluene, but readily soluble in water, methanol, ethanol and acetic acid. Figures 3 and 4 present the high-performance liquid chromatography-mass spectrometry (HPLC-MS) analysis of BBI and BBSIC in the electrospray ionization (ESI) mode. The BBI spectra showed ion at $[M+H]^+$ as a base peak along with ion $[M+Na]^+$ (Fig. 3). The ion $[M-H]^+$ was observed as a base peak in the BBSIC spectra (Fig. 4).

Figure 5 presents TG/DTA curves of BBSIC and two peak are observed on the DTA curve. To reduce water content, BBSIC was dried in a vacuum oven at 100 °C for 12 h prior to experiments. The onset of temperature degradation of BBSIC was observed around 200 °C, and its thermal decomposition ends around 400 °C. The

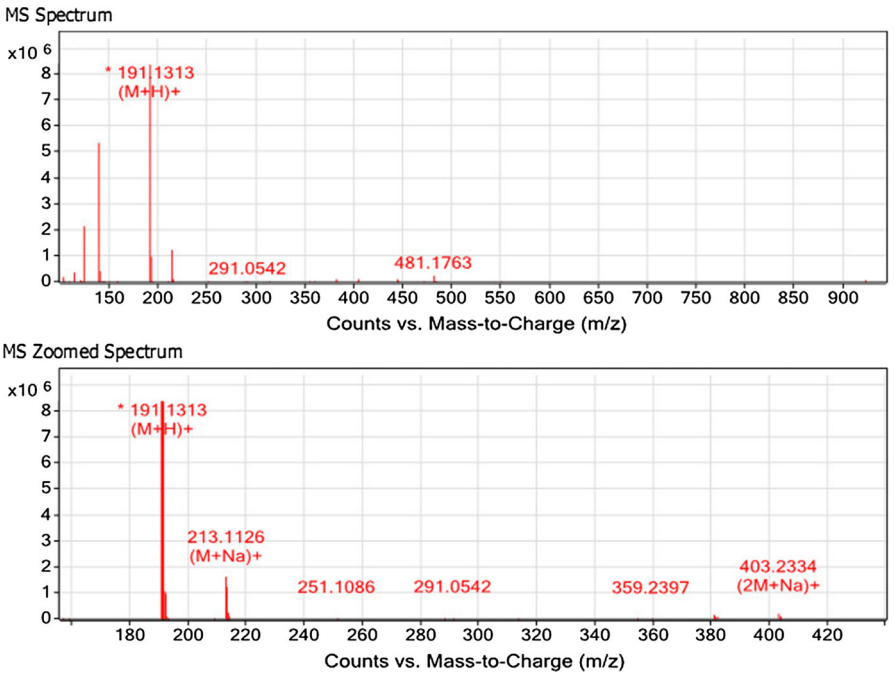

Fig. 3 Detection of $[BBI + H]^+$ ($C_{10}H_{15}N_4^+$) and $[BBI + Na]^+$ ($C_{10}H_{14}N_4Na^+$) ions in BBI by positive ion mode LC–ESI–MS

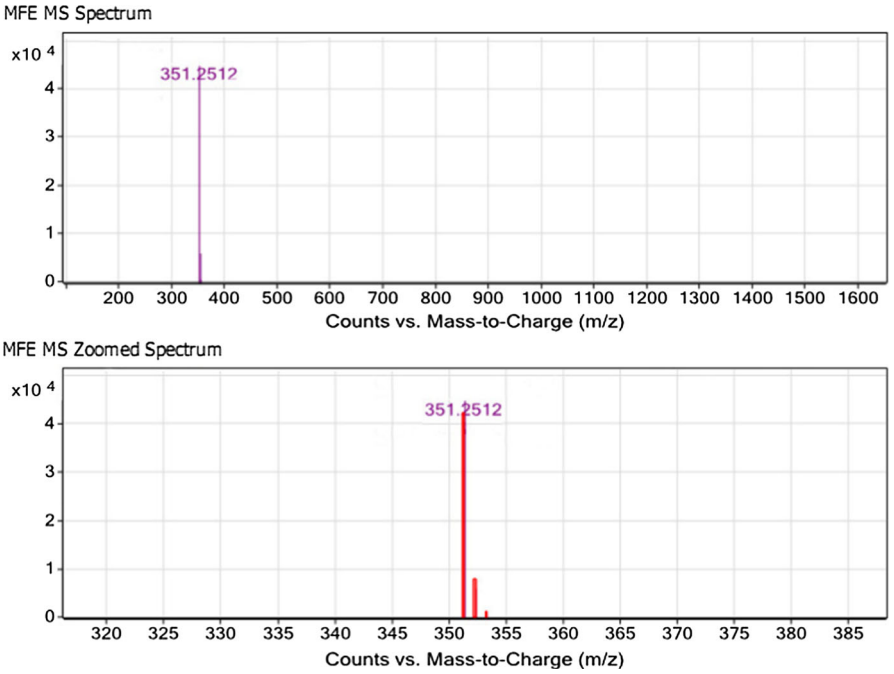

Fig. 4 Detection of $[BBSI]^+$ ($C_{10}H_{15}N_4O_6S_2^+$) ion in BBSI-Cl by positive ion mode LC–ESI–MS

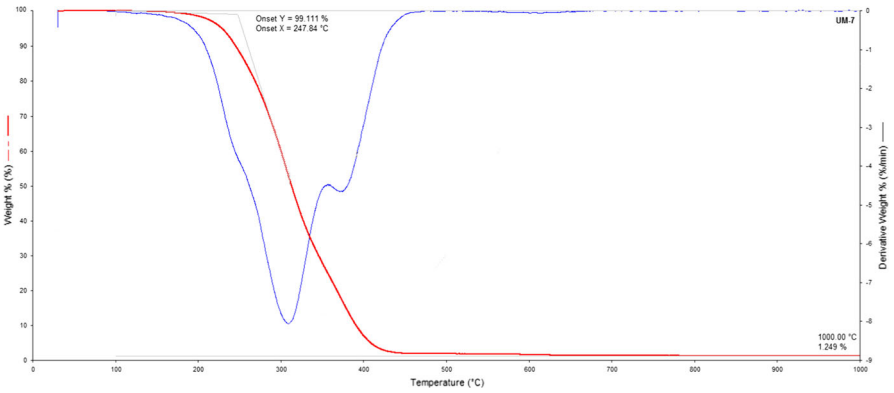

Fig. 5 TG-DTA of BBSIC

results of TG/DTA experiment showed that BBSIC was thermally stable even at relatively high temperatures and its thermal stability can be a consequence of the presence of an imidazole ring and sulfonic groups in the structure of BBSIC. This information is very important from the technological point of view because it provide other useful data such as phase transitions, absorption and desorption; as well as chemical phenomena including chemisorptions, thermal decomposition, and solid-gas reactions viz. oxidation or reduction.

Synthesis of xanthenes in the presence of BBSIC

Initially, the reaction of 4-chlorobenzaldehyde (**1d**) and 5,5-dimethylcyclohexane-1,3-dione (dimedone; **A**) as the model reaction was investigated at room temperature under catalyst- and solvent-free condition. The model reactants were ground using a planetary ball mill to afford the desired product in trace yield at room temperature after 6 h (monitored by LC–MS), confirming demand catalyst for this reaction. Next, the model reactants were taken up in BBSIC as a dual solvent-catalyst reagent and the mixture was stirred for a reaction time of 30 min at room temperature. A minimum amount of water was added to the mixture of reaction and filtered to remove the IL. Then, the crude product was recrystallized from hot ethanol to give the pure product (**2d**) in 47% yield (Table 1, entry 2). When the amount of IL was doubled, yield was improved to 82% (Table 1, entry 3), but further increasing the loading of IL led to no significant improvement in yield (Table 1, entry 4). Decreasing the reaction time at the optimized loading IL results in a decrease in yield (Table 1, entry 5), whereas increasing reaction time improved yield slightly (Table 1, entry 6). The yield was improved to 96% when the model reaction was performed at 50 °C under optimized conditions (Table 1, entry 7). Decreasing the reaction time caused a slight reduction in yield of **2d** at optimal temperature (Table 1, entries 8 and 9).

The scope of the synthesis of 9-(aryl-phenyl)-3,3,6,6-tetramethyl-3,4,5,6,7,9-hexahydro-2*H*-xanthene-1,8-dione (**2**) via this protocol was evaluated by utilizing a variety of aldehydes **1**(**a**–**j**) and dimedone under optimized conditions (Scheme 2).

Aryl aldehydes containing a broad range of substituents were reacted with dimedone under optimized conditions, as shown in Table 2. The aldehydes bearing electron-withdrawing or electron-donating substituents in the aromatic ring gave the

Table 1 Optimization of the synthesis of 9-(4-chloro-phenyl)-3,3,6,6-tetramethyl-3,4,5,6,7,9-hexahydro-2*H*-xanthene-1,8-dione (**2d**) under a variety of reaction conditions[a]

Entry	Loading BBSIC as dual solvent-catalyst (mL)	Temperature (°C)	Reaction time (min)	Yield (%)[b]
1	0	r.t.	360	24[c]
2	1	r.t.	30	47
3	2	r.t.	30	82
4	3	r.t.	30	85
5	2	r.t.	15	74
6	2	r.t.	45	85
7	2	50	30	96
8	2	50	20	92
9	2	50	10	92

[a]Reaction conditions: 4-chlorobenzaldehyde (**1d**; 2.0 mmol), dimedone (4.0 mmol)

[b]Isolated yield

[c]Monitored by LC–MS

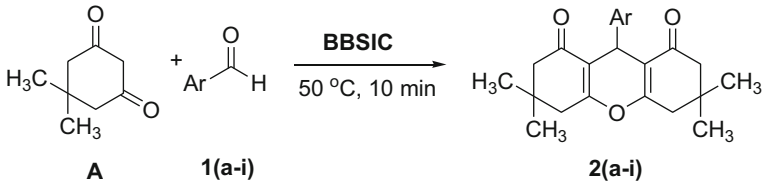

Scheme 2 Synthesis of 1,8-dioxo-octahydroxanthene in the presence of BBSIC under optimal conditions

desired products in good to excellent yields (Table 2). Aldehydes bearing electron-withdrawing substituents afforded a higher yield of **2** than electron-donating substituents at the same position and conditions (Table 2, entries 2 and 3). With electron-withdrawing substituents such as nitro ($-NO_2$) in the *para* position of aryl aldehydes, the electrophilicity of the carbonyl group is enhanced, while electron-donating groups such as methoxy ($-OCH_3$) in the same position clearly decrease the electrophilicity of the carbonyl group. The acid-sensitive aldehydes such as 4-methoxybenzaldehyde, furan-2-carboxaldehyde and cinnamaldehyde afforded the desired product in good yield without any decomposition, by-product and isomerization under the optimized reaction conditions (Table 2, entries 3, 6 and 7). Furthermore, heterocyclic aldehydes such as 2-thiophene carboxaldehyde also gave the desired product in moderate yield (Table 2, entry 8). When the reaction of salicylaldehyde and dimedone was performed under optimized conditions, 9-(2-hydroxy-4,4-dimethyl-6-oxocyclohex-1-enyl)-3,3-dimethyl-2,3,4,9-tetrahydro-1H-xanthen-1-one (**2j**) was obtained in 82% yield (Table 2, entry 9). The structure of this compound was confirmed by physical and spectral data. FTIR, ^{1}H NMR and ^{13}C NMR were in close agreement with that reported in the literature [51, 52]. It was found that the yields and reaction times were apparently affected by the steric hindrance of aryl aldehydes, and the steric hindrance effects seem to be more effective than electronic properties. The sterically hindered aryl aldehyde such as 2,4,6-trimethyl benzaldehyde (**1i**) showed lower reactivity; however, the desired product **2i** was afforded in 67% yield after 30 min (Table 1, entry 10).

The scope of the present protocol was extended by condensation of two equivalents of 2-naphthol and one equivalent of aryl aldehydes containing the electron-withdrawing or electron-donating substituents (Scheme 3). The desired 14-aryl-14*H*-dibenzo[*a,j*]xanthenes were afforded in good to excellent yields in 10 min under aforementioned conditions (Table 2, entries 11–16).

Finally, the synthesis of unsymmetrical xanthenes viz., 12-aryl-8,9,10,12-tetrahydrobenzo[*a*]xanthene-11-ones was performed by condensation of one equivalent of the different aryl aldehydes with one equivalent of dimedone (**A**) and one equivalent of 2-naphthol (**B**; Table 2, entries 17-23; Scheme 4). The obtained results showed the efficiency of this method in the synthesis of both symmetric and unsymmetric xanthenes (Table 2).

The large-scale synthesis of the present protocol was studied by stirring 4-chlorobenzaldehyde (0.05 mol) and dimedone (0.1 mol) in 20 mL of BBSIC at 50 °C. After 30 min, 20 mL of deionized water was added and the suspension was

Table 2 The one-pot synthesis of xanthene derivatives in the presence of BBSIC[a]

Entry	Substrate (**A, B, A** and **B**)	Aldehydes (**1**)	Xanthene (**2**)	Yield (%)[b]	Melting point (°C)	
					Found	Reported [ref.]
1	Dimedone (**A**)	C_6H_5–CHO	a	91	202–204	205–206 [53]
2		4-CH_3–C_6H_4–CHO	b	92	210–213	212–214 [54]
3		4-CH_3O–C_6H_4–CHO	c	88	239–241	241–243 [53]
4		4-Cl–C_6H_4–CHO	d	92	228–230	230–232 [55]
5		4-NO_2–C_6H_4–CHO	e	96	219–221	221–223 [53]
6		Furan-2-carboxaldehyde	f	90[c]	164–166	–
7		Cinnamaldehyde	g	82[c]	175–177	176–178 [56]
8		Thiophene-2-carboxaldehyde	h	88[c]	147–149	–
9		2,4-$(CH_3)_2$–C_6H_3–	i	67[c]	210–212	–
10		Salicylaldehyde	j	82[c]	190 (dec.)	–
11	2-naphthol (**B**)	C_6H_5–CHO	k	92	184–186	185–186 [32]
12		4-CH_3–C_6H_4–CHO	l	90	234–236	224–225 [57]
13		4-CH_3O–C_6H_4–CHO	m	88	205–207	206–208 [32]
14		4-Cl–C_6H_4–CHO	n	92	291–293	293–295 [32]
15		4-NO_2–C_6H_4–CHO	o	96	> 300	310–312 [32]
16		Furan-2-carboxaldehyde	p	87[c]	198–200	202–204 [32]
17	Dimedone (**A**) and 2-naphthol (**B**)	C_6H_5–CHO	q	90	152–154	154–155 [58]
18		4-CH_3–C_6H_4–CHO	r	87	170–172	177 [57]
19		4-CH_3O–C_6H_4–CHO	s	80	202–204	205–206 [56]
20		4-Cl–C_6H_4–CHO	t	90	178–180	181–182 [56]
21		4-NO_2–C_6H_4–CHO	u	93	177–179	180 [58]
22		Thiophene-2-carboxaldehyde	v	84[c]	175–177	–
23		4-$(CH_3)_2CH$–C_6H_4–CHO	w	87	150–152	150–152 [31]

[a]Reaction conditions: aldehyde (**1**; 2 mmol); substrate **A** (4 mmol), **B** (4 mmol), or **A** + **B** (2 mmol + 2 mmol); reaction time (10 min); temperature (50 °C)

[b]Isolated yield

[c]Reaction time was 30 min

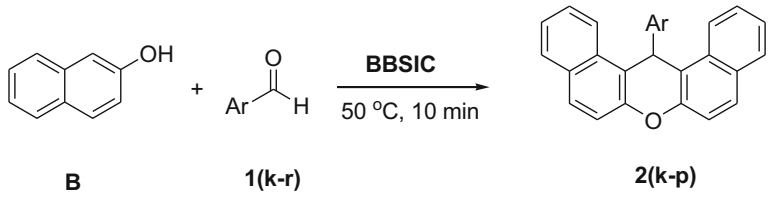

Scheme 3 Synthesis of 14-aryl-14*H*-dibenzo[*a*,*j*]xanthenes in the presence of BBSIC under optimal conditions

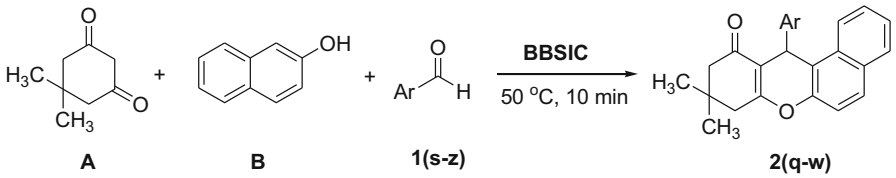

Scheme 4 Synthesis of 12-aryl-8,9,10,12-tetrahydrobenzo[*a*]xanthene-11-ones in the presence of BBSIC under optimal conditions

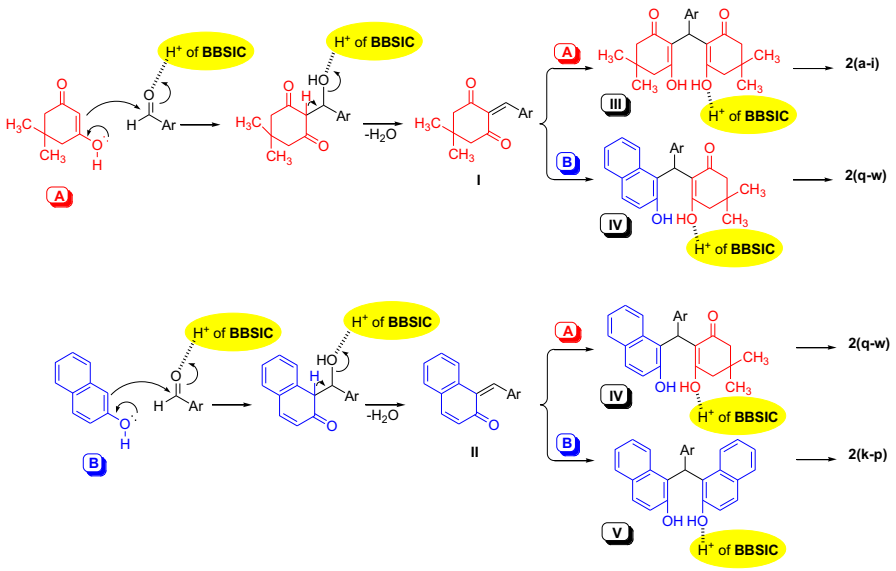

Scheme 5 A plausible mechanism for the synthesis of symmetrical and unsymmetrical xanthenes in the presence of BBSIC

filtered to remove the IL. Then, the crude product was recrystallized from hot ethanol to give the pure product (**2d**) in 77% yield.

Although the mechanism for the current transformation has been reported in the literature [29, 30], a plausible mechanism has been presented in Scheme 5. In the first step, BBSIC as a BAIL catalyzes nucleophilic attack on the carbonyl group by

Table 3 Comparison of the result obtained for the synthesis of symmetric and unsymmetric xanthenes in the presence of BBSIC with those afforded using some of the reported catalysts in literature

Entry	Catalyst	Catalyst loading (%)/temperature (°C)/solvent	**2a**		**2k**		**2q**		Ref.
			Time (min)	Yield (%)	Time (min)	Yield (%)	Time (min)	Yield (%)	
1	Sulfated polyborate	10 wt%/100/solvent-free	3	99	3	99	6	97	[27]
2	BTMA-Br_3	4.8/110/solvent-free	–	–	20	87	–	–	[28]
		4.8/MW(300 W)/solvent-free	–	–	5	90	–	–	
3	SuSA	5.6/80/solvent-free	18	92[a]	35	92	30	91[b]	[31]
4	CAN	5/120/solvent-free	–	–	30	96	30	94	[58]
5	[Et_3N-SO_3H]Cl	25/80–120/solvent-free	60	97	30	96	–	–	[63]
6	[H-NMP][HSO_4]	10/110/solvent-free	–	–	12	94	–	–	[24]
7	[MIMES] in [BMIm][BF_4]	0.08/80/solvent-free	–	–	300	98	–	–	[64]
8	[DBU]$_2$[EDS]	40/120/solvent-free	6	90	7	93	5	92	[65]
9	[NMP][H_2PO_4]	20/80/solvent-free	–	–	–	–	45	86	[66]
10	DSIMHS	25/55–90/solvent-free	4	95	3	94	20	93	[67]
11	[Dsim]Cl	10/110/solvent-free	6	98	5	90	15	85	[68]
12	[MIMPS][HSO_4]	25/100/solvent-free	–	–	7	93	–	–	[69]
13	n-WO_3-SO_3H	19 mg/100/solvent-free	66	92	–	–	8	91	[70]
14	BBSIC	2 mL/50/solvent-free	10	91	10	92	10	90	This work

BTMA-Br_3 = benzyltrimethylammonium tribromide; SuSA = succinimide sulfonic acid; CAN = ceric ammonium nitrate; [NMP] = 1-methyl-2-pyrolidone; [MIMES] = 2,1'-methylimidazolium-3-yl-1-ethylsulfate; [DBU]$_2$[EDS] = ethan-1,2-diyl-bis(hydrogensulfate) and 1,8-diazobicyclo[5.4.0]undec-7-ene; DSIMHS = 1,3-disulfonic acid imidazolium hydrogen sulfate; [Dsim]Cl = 1,3-disulfonic acid imidazolium chloride; [MIMPS][HSO_4] = 1-methyl-3-propanesulfonic-imidazoliumhydrosulfate

[a]4-Chlorobenzaldehyde

[b]4-Isopropylbenzaldehyde

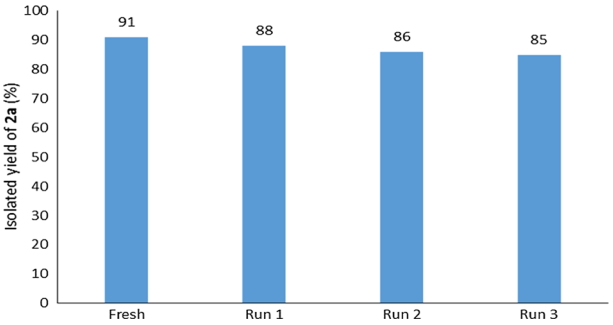

Fig. 6 Comparison of **2a** yield for the fresh and reused BBSIC during three runs under optimal conditions

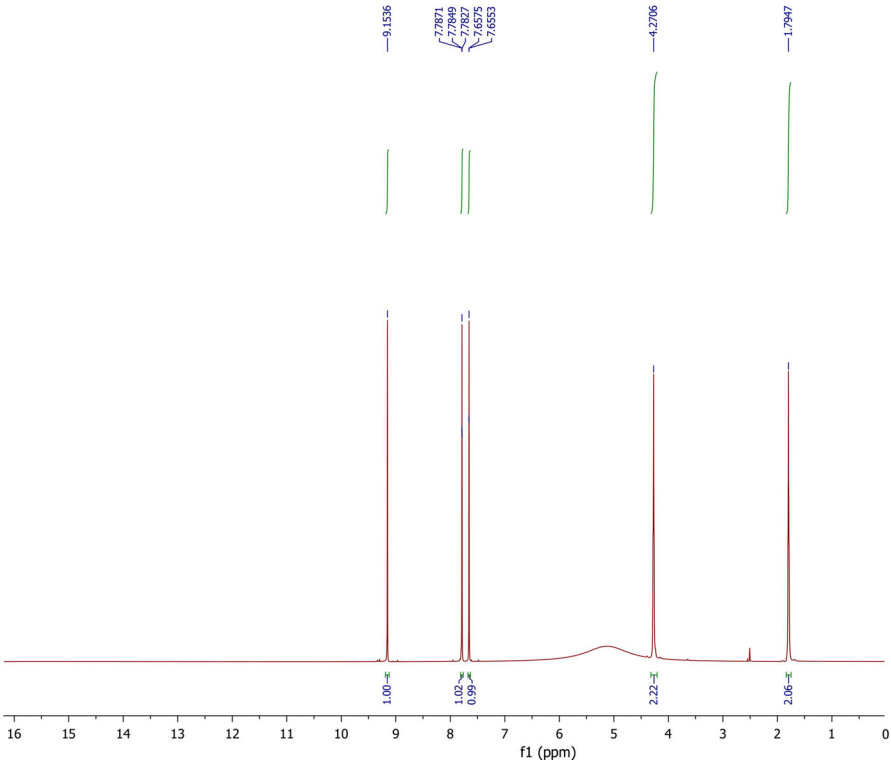

Fig. 7 ^{1}H NMR spectra of reused BBSIC after the third run

dimedone or 2-naphthol. It seems that BBSIC can serve as a dehydrating agent to facilitate the formation of Knoevenagel intermediates (**I**) or (**II**) [61, 62]. Then, Michael addition of a second dimedone or 2-naphthol molecule to intermediates (**I**) or (**II**) follows, and the final product is afforded after intramolecular

cyclodehydration of intermediates (**III**), (**IV**) and (**V**); BBSIC can also facilitate this step.

As one can see in Table 3, the present protocol shows very good comparability with the methods reported in literature when all terms such as yield, reaction time, work-up, mild conditions, catalyst loading, reusability and sustainability are taken into account.

Reusability of BBSIC

ILs can be recovered and reused. Often, the IL can be removed by water from the organic products using a simple workup. In cases in which this procedure cannot be performed, the organic products can be extracted by nonpolar organic solvents and the remaining IL can be concentrated and then directly recharged with new reactants for another run. In the present protocol, after completion of the reaction, the desired xanthenes were readily extracted using ethyl acetate because new IL BBSIC is insoluble in EtOAc and the remaining IL was concentrated under reduced pressure and recharged with new model reactants for another run. The desired product **2a** was obtained at an average 87% yield for three subsequent runs (Fig. 6). The catalytic activity of the recycled liquid acid showed almost no significant loss even after three consecutive runs.

Furthermore, the structure of reused BBSIC was analyzed by ^{1}H NMR in DMSO-d_6 after the third run. As observed in Fig. 7, the chemical structure of BBSIC showed no significant change under the present conditions.

Conclusion

In summary, a new binuclear TSIL was prepared in two steps and its structure was characterized by FTIR, HRMS and ^{1}H and ^{13}C NMR; then, the physical properties and pH of the IL in water was determined. Its dual solvent-catalytic property was proved for the synthesis of symmetric and unsymmetric xanthenes under mild conditions. The current protocol has the advantages of being a simple experimental and sustainable procedure, with good yield of the desired products within short reaction times, and recyclability of the IL. Its application in the synthesis of xanthenes highlights the importance of TSILs in organic chemistry, and we hope that the current work will encourage further research in this area.

Acknowledgements This work was supported by a "High Impact Research Grant" (no. RP025A/B/C-14AET) for Scientific Research from University of Malaya, Malaysia. The authors are grateful to staff members in the Analytical and Testing Center of Research House of Professor Reza and the University of Malaya for partial support.

References

1. A.S. Amarasekara, Chem. Rev. **116**, 6133 (2016)
2. D.D. Patel, J.M. Lee, Chem. Rec. **12**, 329 (2012)
3. X. Sun, H. Luo, S. Dai, Chem. Rev. **112**, 2100 (2012)

4. R.L. Vekariya, J. Mol. Liq. **227**, 44 (2017)
5. X. Cai, Q. Wang, Y. Liu, J. Xie, Z. Long, Y. Zhou, J. Wang, A.C.S. Sustain, Chem. Eng. **4**, 4986 (2016)
6. N.G. Khaligh, Res. Chem. Intermed. **41**, 5411 (2015)
7. N.G. Khaligh, Polycycl. Aromat. Compd. **36**, 284 (2016)
8. N.G. Khaligh, Chin. J. Catal. **35**, 1036 (2014)
9. N.G. Khaligh, Chin. J. Catal. **35**, 1497 (2014)
10. R.L. Vekariya, N.S. Kumar, Coll. Surf. A **529**, 203 (2017)
11. R.L. Vekariya, A. Dhar, J. Lunagariya, Compos. Interface **24**, 801 (2017)
12. H. Olivier-Bourbigou, L. Magna, J. Mol. Catal. A Chem. **182–183**, 419 (2002)
13. Z.S. Qureshi, K.M. Deshmukh, B.M. Bhanage, Clean Technol. Environ. **16**, 1487 (2014)
14. Y. Mori, I. Fujita, H. Kawabe, K. Fujita, T. Tanaka, A. Kishimoto, Analyst **111**, 1409 (1986)
15. Y. Kushida, T. Nagano, K. Hanaoka, Analyst **140**, 685 (2015)
16. Y. Hori, K. Nakaki, M. Sato, S. Mizukami, K. Kikuchi, Angew. Chem. Int. Ed. **51**, 5611 (2012)
17. H.N. Hafez, M.I. Hegab, I.S. Ahmed-Farag, A.B.A. El-Gazzar, Bioorg. Med. Chem. Lett. **18**, 4538 (2008)
18. J.J. Omolo, M.M. Johnson, S.F. van Vuuren, C.B. De Koning, Bioorg. Med. Chem. Lett. **21**, 7085 (2011)
19. A.M. El-Brashy, M. El-Sayed Metwally, F.A. El-Sepai, Il Farmaco **59**, 809 (2004)
20. C.P. Wu, D.A. van Schalkwyk, D. Taylor, P.J. Smith, K. Chibale, Int. J. Antimicrob. Agents **26**, 170 (2005)
21. K. Chibale, M. Visser, D. van Schalkwyk, P.J. Smith, A. Saravanamuthu, A.H. Fairlamb, Tetrahedron **59**, 2289 (2003)
22. A.K. Bhattacharya, K.C. Rana, M. Mujahid, I. Sehar, A.K. Saxena, Bioorg. Med. Chem. Lett. **19**, 5590 (2009)
23. R. Giri, J.R. Goodell, C. Xing, A. Benoit, H. Kaur, H. Hiasa, D.M. Ferguson, Bioorg. Med. Chem. **18**, 1456 (2010)
24. H. Naeimi, Z.S. Nazifi, C. R. Chimie **17**, 41 (2014)
25. M. Dabiri, M. Baghbanzadeh, M.S. Nikcheh, E. Arzroomchilar, Bioorg. Med. Chem. Lett. **18**, 436 (2008)
26. B. Rajitha, B.S. Kumar, Y.T. Reddy, P.N. Reddy, N. Sreenivasulu, Tetrahedron Lett. **46**, 8691 (2005)
27. M.S. Patil, A.V. Palav, C.K. Khatri, G.U. Chaturbhuj, Tetrahedron Lett. **58**, 2859 (2017)
28. U. Kusampally, R. Pagadala, C.R. Kamatala, Tetrahedron Lett. **58**, 3316 (2017)
29. N.G. Khaligh, Ultrason. Sonochem. **19**, 736 (2012)
30. N.G. Khaligh, Catal. Sci. Technol. **2**, 2211 (2012)
31. F. Shirini, N.G. Khaligh, Dyes Pigm. **95**, 789 (2012)
32. N.G. Khaligh, F. Shirini, Ultrason. Sonochem. **22**, 397 (2015)
33. D. Prasad, A. Preetam, M. Nath, C. R. Chimie **15**, 675 (2012)
34. M.A. Naik, D. Sachdev, A. Dubey, Catal. Commun. **11**, 1148 (2010)
35. A. Hassner, *Synthesis of Heterocycles via Cycloadditions II* (Springer, Berlin Heidelberg, 2008)
36. N.G. Khaligh, J. Mol. Catal. A Chem. **349**, 63 (2011)
37. N.G. Khaligh, Catal. Sci. Technol. **2**, 1633 (2012)
38. N.G. Khaligh, Chin. Chem. Lett. **26**, 26 (2015)
39. N.G. Khaligh, Monatsh. Chem. **145**, 1643 (2014)
40. N.G. Khaligh, Monatsh. Chem. **146**, 321 (2015)
41. N.G. Khaligh, Polycycl. Arom. Compd. **35**, 428 (2015)
42. G.H. Silver, J.L. Wood, Trans. Faraday Soc. **60**, 5 (1964)
43. R. Ramasamy, J. Appl. Spec. **80**, 492 (2013)
44. R. Ramasamy, Arm. J. Phys. **8**, 51 (2015)
45. V. Krishnakumar, R. Ramasamy, Indian J. Pure Appl. Phys. **40**, 252 (2002)
46. N.P.G. Roeges, *A Guide to the Complete Interpretation of Infrared Spectra of Organic Structures* (Wiley, New York, 1994)
47. S.M. Chackalackal, F.E. Stafford, J. Am. Chem. Soc. **88**, 4815 (1966)
48. R.T. Conley, *Infrared Spectroscopy* (Allyn and Bacon Inc., Boston, 1966)
49. K. Nakamoto, *Infrared and Raman Spectra of Inorganic and Coordination Compounds* (Wiley, N.Y., 1986)
50. C.N.R. Rao, Can. J. Chem. **42**, 36 (1964)
51. L. Jurd, J. Org. Chem. **31**, 1639 (1966)

52. Y.L. Li, X.S. Wang, D.Q. Shi, S.J. Tu, Y. Zhang, Acta Cryst. **E60**, o1439 (2004)
53. K. Venkatesan, S.S. Pujari, R.J. Lahoti, K.V. Srinivasan, Ultrason. Sonochem. **15**, 548 (2008)
54. A. Ilangovan, S. Muralidhara, P. Sakthivel, S. Malayappasamy, S. Karuppusamy, M.P. Kaushik, Tetrahedron Lett. **54**, 491 (2013)
55. S. Kokkirala, N.M. Sabbavarapu, V.D.N. Yadavalli, Eur. J. Chem. **2**, 272 (2011)
56. G.H. Mahdavinia, M.A. Bigdeli, Y. Saeidi, Hayeniaz. Chin. Chem. Lett. **20**, 539 (2009)
57. F. Shirini, N.G. Khaligh, G.H. Imanzadeh, P.G. Ghasem-Abadi, Chin. Chem. Lett. **23**, 1145 (2012)
58. A. Kumar, S. Sharma, R.A. Maurya, J. Sarkar, J. Comb. Chem. **12**, 20 (2010)
59. J.M. Khurana, D. Magoo, Tetrahedron Lett. **50**, 4777 (2009)
60. G.C. Nandi, S. Samai, R. Kumar, M.S. Singh, Tetrahedron **65**, 7129 (2009)
61. A.C. Flores, E.A. Flores, E. Hernández, L.V. Castro, A. García, F. Alvarez, F.S. Vázquez, J. Mol. Liq. **196**, 249 (2014)
62. M. Krannich, F. Heym, A. Jess, J. Chem. Eng. Data **61**, 1162 (2016)
63. A. Zare, A.R. Moosavi-Zare, M. Merajoddin, M.A. Zolfigol, T. Hekmat-Zadeh, A. Hasaninejad, A. Khazaei, M. Mokhlesi, V. Khakyzadeh, F. Derakhshan-Panah, M.H. Beyzavi, E. Rostami, A. Arghoon, R. Roohandeh, J. Mol. Liq. **167**, 69 (2012)
64. H. Wu, X. Chen, Y. Wan, H. Xin, H. Xu, C. Yue, L. Pang, R. Ma, Synth. Commun. **39**, 3762 (2009)
65. B. Maleki, E. Akbarzadeh, S. Babaee, Dyes Pigments **123**, 222 (2015)
66. H. Singh, S. Kumari, J.M. Khurana, Chin. Chem. Lett. **25**, 1336 (2014)
67. F. Shirini, A. Yahyazadeh, K. Mohammadi, Chin. Chem. Lett. **25**, 341 (2014)
68. M.A. Zolfigol, V. Khakyzadeh, A.R. Moosavi-Zare, A. Zare, S.B. Azimi, Z. Asgari, A. Hasaninejad, C. R. Chimie **15**, 719 (2012)
69. K. Gong, D. Fang, H.L. Wang, X.L. Zhou, Z.L. Liu, Dyes Pigm. **80**, 30 (2009)
70. A. Amoozadeh, S. Rahmani, J. Mol. Catal. A: Chem. **396**, 96 (2015)